Solid State Ionics 439 (2026) 117176

Contents lists available at ScienceDirect

Solid State Ionics

journal homepage: www.elsevier.com/locate/ssi

Single-crystal layer-structured metal oxide cathode material for high-voltage sodium ion batteries

Pavithra Kamatchisundaram [a,*], Meyyappan Revathi [a,*], S. Bala Abirami [b]

[a] Department of Chemistry, Vels Institute of Science, Technology and Advanced Studies, Pallavaram, Chennai 600117, India
[b] Department of Condensed Matter Physics, Saveetha School of Engineering, Saveetha Institute of Medical and Technical Sciences (SIMATS), Chennai 602105, Tamil Nadu, India

ARTICLE INFO

Keywords:
Single crystal
Solid-state method
Layered structure
High-voltage cathode
Sodium-ion battery

ABSTRACT

High-voltage cathodes offer increased energy density and rate capacity, which qualifies sodium ion batteries (SIBs) for high-power applications. Since, transition metal oxide layered type cathodes are the most promising candidates for sodium ion batteries. Recently, metal oxide layered single crystal materials have gained greater attention as cathodes because of their high voltage capabilities. Herein, we report a single-crystal layer structured P2-typed $Na_{0.66}Ni_{0.33}Mn_{0.67}O_2$ (P2-NNM) oxide cathode material, synthesized via a high-temperature solid-state method for high-voltage sodium-ion battery applications. Microscopic investigations clearly reveal the single crystal morphology of the material, and X-ray diffraction pattern confirms the P2 phase with a high degree of crystallinity. The observed lattice spacing of the single-crystal material is 0.562 nm. Electrochemical studies of the cathode material unveil outstanding specific capacity of 170 and 218 mAh g^{-1} at 0.1C, when cycled up to 4.5 and 5.0 V respectively. These results highlight the importance of developing of high- voltage single-crystal layered cathode materials, and open a path way toward high-energy density sodium-ion battery applications.

1. Introduction

There is a constant need for sustainable battery systems that can store and provide electricity in a clean and sustainable manner. As the world warms and moves away from fossil fuels toward electric vehicles (EVs) that needs higher safety and endless performances [1]. It is anticipated that by 2030, there will be 25 million electric vehicles powered by conventional lithium-ion batteries (LIBs) worldwide [2]. However, the rapidly increasing demand for lithium resources, coupled with their limited and uneven global distribution, has led to rising concerns regarding resources availability and cost. The sodium-ion batteries (SIBs) on the other hand, are currently being employed for huge in electric mobility and large-scale applications due to the growing demand for more efficient and affordable way [3–5]. This is due to the fact that sodium precursors are less expensive and more common than lithium [6–8], and they are also similarly distributed across the Earth's crust. Accordingly, similar chemical properties, various lithium-based analogue electrode materials have been proposed as cathodes for SIBs. As a result, numerous other sodium-based cathode materials, such as layered oxides, organic compounds, and polyanionic materials (phosphates, pyrophosphates, and mixed polyanions), have been extensively investigated [9–11]. Despite these advances, the commercialization of SIBs remains hindered by key challenges, particularly limited cycle life and relatively low energy density which is need to be addressed. The electrochemical performance of SIBs can be enhanced by cathode materials. According to recent study the high-voltage cathodes provide a better energy density and rate capacity, which makes SIBs appropriate for high power applications [12].The layered transition metal oxides show outstanding rate performance and cycling stability due to their enormous sodium layer spacing, which enhances ion transport [13]. However, regardless of these advantages, layered cathode materials encounter significant challenges at high voltage operations. For example, conventional P2-type layered transition metal-oxide cathode can undergo a P2-O2 phase transition at 4.2 V and above, that triggering lattice parameter changes which lead to capacity degradation [14]. Accordingly, stabilizing cathode materials during high-voltage operations is a key strategy for the development of next-generation sodium ion batteries. To improve energy density while preserving high-voltage stability, previous studies have established a range of functional approaches, including elemental doping, modified synthesis

* Corresponding authors.
E-mail addresses: pavithrasundaram81@gmail.com (P. Kamatchisundaram), mrev80@gmail.com (M. Revathi).

https://doi.org/10.1016/j.ssi.2026.117176
Received 24 November 2025; Received in revised form 9 February 2026; Accepted 27 February 2026
Available online 14 March 2026

methods, and surface coatings. These strategies aim to enhance both the electrochemical performance and structural stability of cathode materials to increase the operating voltage [15]. Moreover, additional strategies include tailoring the electrolyte composition with advanced additives, introduce inactive element dopants or modifying the cathode surface to improve interfacial compatibility during high voltage operation has also been reported as an effective strategy [16–18]. In this context self-supported 3D porous structures developed via electrostatic spray deposition (ESD) have attracted attention, as they can enhance redox activity and enable higher operating voltages with enhanced cycling stability [19]. Significantly, the morphology of the cathode material can also influence the efficiency of coating and doping strategies. Well-organized and highly crystallized structures facilitate improved ion diffusion and more stable electrochemical performance at high voltage [20]. In recent years, single-crystal structure based NMC materials for lithium ion batteries have fascinated widespread attention from both industry and academia, owing to their advantages in material reliability, cycling performance, thermal stability, and high operating voltage compared with conventional NMC materials [21]. However in the case of sodium ion batteries only limited reports are available on high voltage P2-layered cathode materials [22–28].Although noteworthy progress has been made in recent years toward improving the high-voltage stability of sodium cathode materials, significant challenges still persist, particularly in further enhancing the overall cell performance.

In this work, we report the design of a high-voltage sodium-ion battery cathode, based on a single-crystal P2- type layered transition-metal oxide material with improved crystallinity and phase purity. The structural and electrochemical properties of the cathode were evaluated in half-cell configuration, and the corresponding results are discussed.

2. Materials and methods

A two-step solid-state reaction method was employed for the preparation of P2-type $Na_{0.66}Ni_{0.33}Mn_{0.67}O_2$ using stoichiometric amounts of acetate-based precursors. Sodium acetate dihydrate $Na(CH_3COO)\cdot 4H_2O$ (Alfa Aesar, 99.95%), nickel acetate tetrahydrate $Ni(CH_3COO)_2\cdot 4H_2O$, and manganese acetate tetrahydrate $Mn(CH_3COO)_2\cdot 4H_2O$ (Alfa Aesar, 98%) were used as received without further purification. In order to achieve homogeneous cation distribution and phase-pure single-crystal formation, acetate precursors were selected for the synthesis of the P2-NNM cathode due to their good solubility and ability to ensure uniform mixing of metal ions at the molecular level. Upon thermal treatment, acetate salts decompose cleanly into their corresponding oxides, releasing volatile by-products without leaving residual impurities, which facilitates uniform cation distribution and phase purity. [4,7] Typically, 0.66 g of $Na(CH_3COO)\cdot 4H_2O$, 0.33 g of $Ni(CH_3COO)_2\cdot 4H_2O$, and 0.67 g of $Mn(CH_3COO)_2\cdot 4H_2O$ were thoroughly mixed using a high-energy planetary ball mill (RETSCH PM-100) at 250 rpm for 2 h to obtain a homogeneous fine powder and enhance metal ion diffusion.

Subsequently, the mixed powders were calcined at 900 °C with a heating rate of 3 °C min^{-1} and maintained for 12 h. After natural cooling to room temperature, the obtained oxide powders were ground using an agate mortar and pestle to yield the final product. The resulting single-crystal P2-type $Na_{0.66}Ni_{0.33}Mn_{0.67}O_2$ material is hereafter referred to as P2-NNM and was used for further material characterization and electrochemical measurements. The formation of the single-crystal P2-NNM material is primarily governed by the high-temperature calcination and precursor homogeneity. The use of stoichiometrically balanced acetate precursors, combined with high-energy ball milling, ensures uniform elemental distribution prior to calcination. A high calcination temperature of 900 °C, along with a slow heating rate (3 °C min^{-1}) and prolonged dwelling time (12*h*), promotes sufficient atomic diffusion and grain growth, thereby suppressing grain boundary formation and favoring single-crystal particle evolution. These controlled synthesis conditions collectively contribute to the formation of the well-crystallized single-crystal layered structure.

2.1. Electrochemical characterization

In an Ar-filled glove box (Laplux 2000), CR2032-type half-cells were fabricated using the prepared material as the cathode and sodium metal as the anode. The cathode slurry comprised 92 wt% active material (P2-NNM), 5 wt% conductive carbon black (Super P, 99%, Alfa Aesar), and 3 wt% polyvinylidene difluoride (PVDF) binder (Alfa Aesar, 98%).To remove volatile components, the slurry was coated onto aluminum (Al) foil (16 μm thickness) and dried at 85 °C overnight in a vacuum oven. The average mass loading of the electrodes was approximately 12 mg cm^{-2}. The electrolyte consisted of 1 M $NaPF_6$ (sodium hexafluorophosphate, Alfa Aesar, 99.95%) dissolved in a mixture of ethylene carbonate and propylene carbonate (EC/PC = 1:1, wt%). A polymer composite membrane was used as the separator [29].

2.2. Material characterization techniques

Thermogravimetric analysis (TGA) was performed to gain insight into the crystallization behavior and to determine the optimal temperature for layered structure formation, using a heating rate of 10 °C min^{-1} (PerkinElmer STA-8000). The crystal structure and phase purity of the materials were examined by powder X-ray diffraction (XRD) using a SmartLab SE X-ray diffractometer (Rigaku, Japan) with Cu Kα radiation (λ = 1.540 Å) over a 2θ range of 10–80°. Rietveld refinement was carried out to extract detailed structural parameters. Surface morphology and elemental composition were investigated using a scanning electron microscope (SEM, Quattro S, Thermo Fisher Scientific, USA) equipped with energy-dispersive X-ray spectroscopy (EDS) for elemental mapping. The grain size and selected area electron diffraction (SAED) patterns were obtained using a high-resolution transmission electron microscope (HRTEM, JEOL, Japan). The surface chemical states of the constituent elements in the as-prepared material were analyzed by X-ray photoelectron spectroscopy (XPS) using an ESCALAB 250Xi spectrometer (Thermo Fisher Scientific, Waltham, MA, USA) with Al Kα radiation.The electrochemical impedance technique is executed at a 10 Hz-10 kHz frequency range. Galvano static cyclic performances were analyzed by constant volt & current mode; all the studies were performed using an SP-300 Electrochemical analyzer (Bio-Logic, France).

3. Results

3.1. Material characterizations

To elucidate the formation process of the single-crystal material from precursor to final product during calcination, thermogravimetric analysis (TGA) was carried out, and the corresponding results are presented in Fig. 1(a). An initial weight loss of approximately 20% is observed in the temperature range of 80–130 °C, accompanied by a prominent endothermic peak at around 105 °C. This loss is attributed to the removal of physically adsorbed water and the release of CO_2. In the second stage, within the temperature range of 300–420 °C, three mild endothermic peaks are observed, corresponding to a cumulative weight loss of about 55%. This stage is associated with the decomposition and transformation of the acetate precursors into the P2-NNM phase, which is completed at approximately 420 °C. No significant weight loss is detected beyond 420 °C up to about 850 °C, except for a weak endothermic feature, suggesting that this temperature range is critical for the complete conversion of the oxide phase into a single-crystal layered hexagonal structure [30,31]. A similar thermal behavior has been reported for layered lithium nickel–manganese–cobalt oxide (NMC) materials [32]. The total experimental weight loss (~55%) is closely matches the theoretical weight loss expected from the acetate precursors to the formation of the single-crystal P2-NNM material. The X-ray

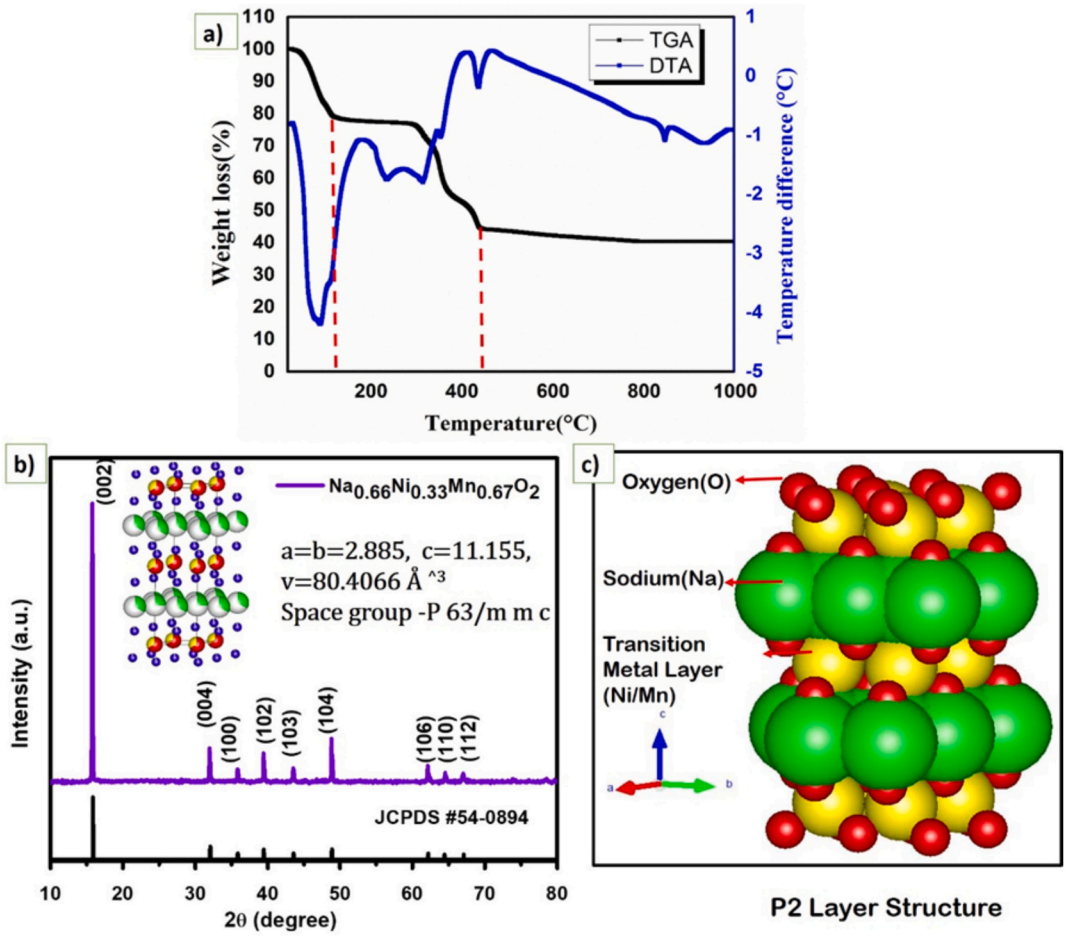

Fig. 1. (a) TGA/DTA profiles of the prepared P2-NNM material, illustrating the thermal decomposition of precursors and oxide phase formation. (b) X-ray diffraction pattern of the single-crystal P2-NNM material, indexed to a hexagonal $P6_3/mmc$ structure (JCPDS No. 54–0894). (c) Schematic illustration of the P2-type layered crystal structure.

diffraction (XRD) pattern of the P2-NNM material, shown in Fig. 1(b), confirms the formation of a highly crystallized P2-layered structure without any detectable impurity phases. All diffraction peaks can be well indexed to a hexagonal symmetry with space group $P6_3/mmc$ (JCPDS No. 54–0894). Notably, no diffraction peaks corresponding to $NiMnO_4$ or other secondary phases are observed, further verifying the high phase purity and single-crystalline nature of the synthesized P2-NNM material. Rietveld refinement was carried out to determine the structural parameters, yielding lattice constants of $a = b = 2.885$ Å and $c = 11.155$ Å, with a unit cell volume of 80.4066 $Å^3$. The presence of nickel in the transition-metal oxide layer is known to influence the lattice parameters and expand the unit cell volume, which is consistent with previous reports [33].The surface morphology, actual grain size, and lattice fringes of the P2-NNM material were examined using SEM and (HR)TEM analyses, with representative images presented in Fig. 2 (a–f). The SEM images reveal well-defined hexagonal particles with a dense morphology and no visible porosity, indicating the formation of single-crystal particles. This observation is further corroborated by HR-TEM images (Fig. 2d,e), which clearly demonstrate the highly ordered crystalline nature of the P2-NNM material.The size of single crystal is around a few hundred nanometers to a few micrometers, as 200 nm to 5 μm.

HR-TEM images of the prepared P2-NNM material reveal a well-defined single- crystalline nature were evidenced by uniform lattice fringes additionally by the interlayer spacing of 0.562 nm, which corresponds to the (002) diffraction plane of X-ray diffraction pattern (Fig. 2(f)) [34]. The elemental mappings of the P2-NNM material are shown in Fig. 2(g) where the mapping analysis reveals a homogeneous distribution of the constituent elements (Na, Ni, Mn, and O) within the layered structure. Furthermore the corresponding EDX-spectrum (Fig. 2 (h)) confirms the presence of all constituent elements, indicating their uniform dispersion throughout the single-crystalline P2-NNM material.

The surface chemical states of the elements present in the P2-NNM electrode material were investigated using X-ray photoelectron spectroscopy (XPS), as shown in Fig. 3. Fig. 3(a) displays the Na 1 s spectrum, which exhibits a single symmetric peak centered at a binding energy of 1071.04 eV, confirming the presence of Na in the P2-type layered structure [35,36].

The Ni 2p core-level spectrum (Fig. 3(b)) shows two prominent peaks located at binding energies of 854.4 and 872.2 eV, corresponding to the Ni $2p_{3/2}$ and Ni $2p_{1/2}$ spin–orbit components, respectively, along with their characteristic satellite features. The presence of these satellite peaks is a typical fingerprint of Ni-based layered oxide cathode materials and is consistent with previously reported results [51,52].Fig. 3(c) presents the Mn 2p spectrum, where the Mn $2p_{3/2}$ and Mn $2p_{1/2}$ peaks appear at binding energies of 642.3 and 653.7 eV, respectively. These binding energy positions are in good agreement with the Mn^{4+} oxidation state commonly observed in layered oxide cathodes [37,38]. The O 1 s spectrum shown in Fig. 3(d) exhibits a dominant peak centered at approximately 529.5 eV, which can be attributed to lattice oxygen associated with metal–oxygen bonds such as Ni—O and Mn—O. A slight asymmetry toward higher binding energy suggests the possible contribution of surface-related oxygen species [39–44].

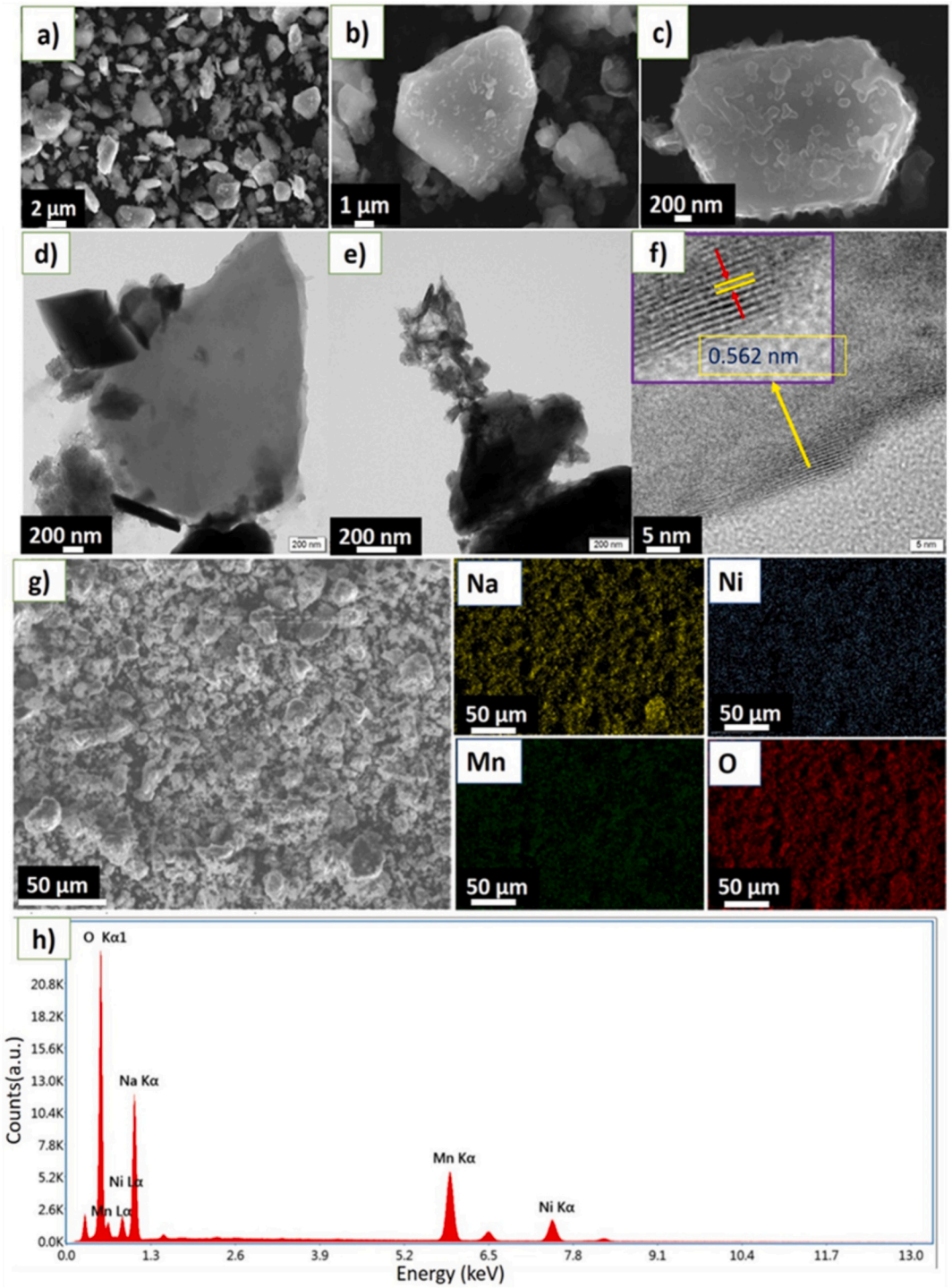

Fig. 2. Electron microscopic analysis of P2-NNM material. (a–c) SEM images at different magnifications showing the morphology of the P2-NNM particles. (d, e) TEM images confirming the single-crystal nature of the particles. (f) HRTEM image displaying clear lattice fringes with an interplanar spacing of 0.562 nm, corresponding to the (002) plane of the P2 layered structure. (g) SEM image and corresponding EDX elemental mapping of Na, Ni, Mn, and O, indicating homogeneous elemental distribution. (h) EDX sum spectrum confirming the elemental composition of the P2-NNM material.

3.2. Electrochemical analytics

Galvanostatic charge-discharge analysis was performed at 0.1C using the prepared single- crystal P2-NNM cathode material within two different cut-off voltage ranges of 1.5–5.0 V and 1.5–4.5 V. Fig. 4(a), when cycled between 1.5 and 5.0 V, the material delivered a high specific discharge capacity of 218 mAh g^{-1} at 0.1C. When cycled between 1.5 and 5.0 V the P2-NNM, exhibited an almost smooth discharge profile with noticeable damping in the charge curve upon reaching the upper cut-off voltage. This change in the charge curve indicates structural deformation in P2-NNM during the charging process. In contrast the smooth discharge behavior indicating stabilization of the P2 structure due to it's single crystalline nature, which also favors a solid-solution-type sodium storage mechanism [45].The high-capacity and wide operating voltage window of P2-NNM are attributed to it's single-crystral nature and the optimized electrolyte composition (1 M $NaPF_6$

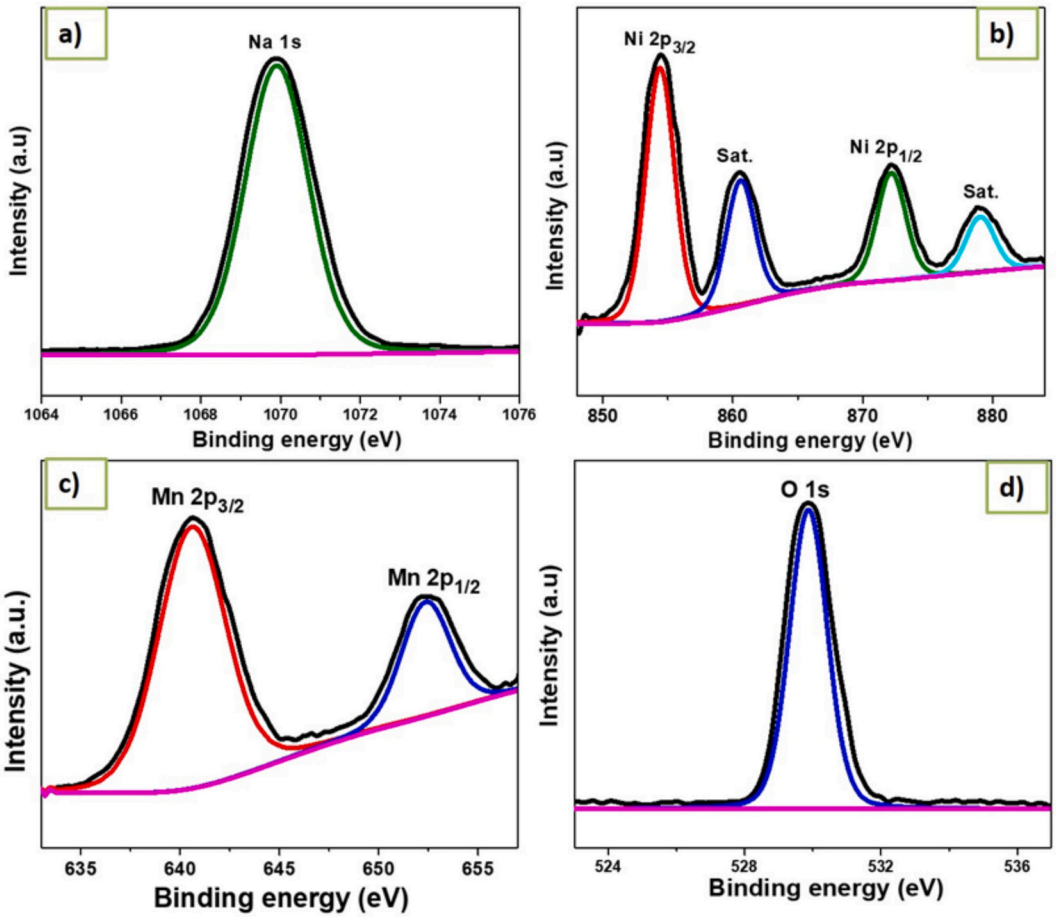

Fig. 3. XPS spectra of the P2-NNM material showing the core-level regions of (a) Na 1 *s*, (b) Ni $2p_{3/2}$ and $2p_{1/2}$, (c) Mn $2p_{3/2}$ and $2p_{1/2}$, and (d) O 1 *s*.

in EC/PC (1:1 wt%)).This performance is superior to that reported for the same material synthesized via different methods and tested in alternative electrolytes, such as 1 M $NaClO_4$ dissolved in propylene carbonate (PC) with 2 vol% fluoroethylene carbonate (FEC)) [46]. Therefore, both the electrolyte.

Composition and synthesis method play critical roles in determining the electrochemical performances of this layered material. However, the P2-NNM material delivered an average coulombic efficiency (CE) of ~98% over 50 cycles at different C-rates. Capacity fading mainly occur when the cells are operated with a high cut-off voltage of 5.0 V Fig. 1, 2, 3 and 4(c), which can be attributed to the occurrence of P2–O2 phase transformation, electrolyte decomposition, and redox reactions of the Mn^{4+}/Mn^{3+} ionic pair, as well as P2–P2′ phase transformation [9,47].To confirm the structural stability of the P2-NNM material after high-voltage cycling, X-ray diffraction (XRD) analysis was performed on the electrode after cycling at 5.0 V. No noticeable change in the layered structure of P2-NNM was observed, indicating that the material remains structurally stable and suitable for high-voltage operation. This stability is attributed to the beneficial incorporation of Ni, which reinforces O (2p)–Mn (3d) hybridization, resulting in reduced Jahn–Teller distortion at the MnO_6 octahedral sites, shorter transition-metal–oxygen slabs, and wider Na-layer spacing [48]. The enhanced high-voltage stability of the single-crystal P2-NNM cathode can be linked to the mitigation of Jahn–Teller (*J*–T) distortion at MnO_6 octahedral sites. In Mn-containing layered oxides, the presence of Mn^{3+} can trigger *J*–T distortion, leading to anisotropic Mn—O bond lengths and local lattice strain during Na^+ extraction/insertion, particularly at high states of charge. This accumulated strain can promote structural rearrangements, accelerate phase transitions, and contribute to capacity fading under high-voltage operation. In a single-crystal morphology, the reduced grain-boundary density and improved crystallographic coherence help suppress stress concentration and crack formation, thereby improving structural tolerance at high voltage and indirectly reducing the impact of *J*–T-driven distortion. Similar relationships between local structural distortion/strain and high-voltage stability in layered oxide cathodes have been discussed in the previous studies [49]. Overall, when the material was operated under different voltage ranges, only minor variations in the discharge voltage were observed. However, further optimization of the electrolyte is required for stable high-voltage operation, which will be addressed in future work. The P2-NNM cathode delivered a discharge capacity of 170 mAh g^{-1} at 0.1C within a potential window of 1.5–4.5 V. Notably, P2-NNM exhibited excellent cycling stability, retaining 91% of its capacity after 50 cycles Fig. 4(c), along with good rate performance. This behavior is attributed to the thermodynamically favorable solid-solution reaction mechanism in the P2-NNM material [47,48]. After 100 cycles (Fig. S1), the electrode still delivered a discharge capacity of 129 mAh g^{-1}, demonstrating its structural robustness during prolonged cycling. The electrochemical performance achieved in this work is superior to that reported for the same material using different electrolytes [46]. However, when operated at a high cut-off voltage of 5.0 V, the electrolyte undergoes decomposition, resulting in unstable cycling behavior and a reduced capacity retention of only 56% after 50 cycles. Impedance analysis was performed over a frequency range of 10 kHz to 10 Hz to examine ionic transport through the cell before and after cycling; the corresponding Nyquist plot is shown in Fig. 4(d). The semicircle observed in the high-frequency region of the impedance plot indicates enhanced Na-ion diffusion capabilities, while the inclined line in the low-frequency region represents Na-ion diffusion across cells

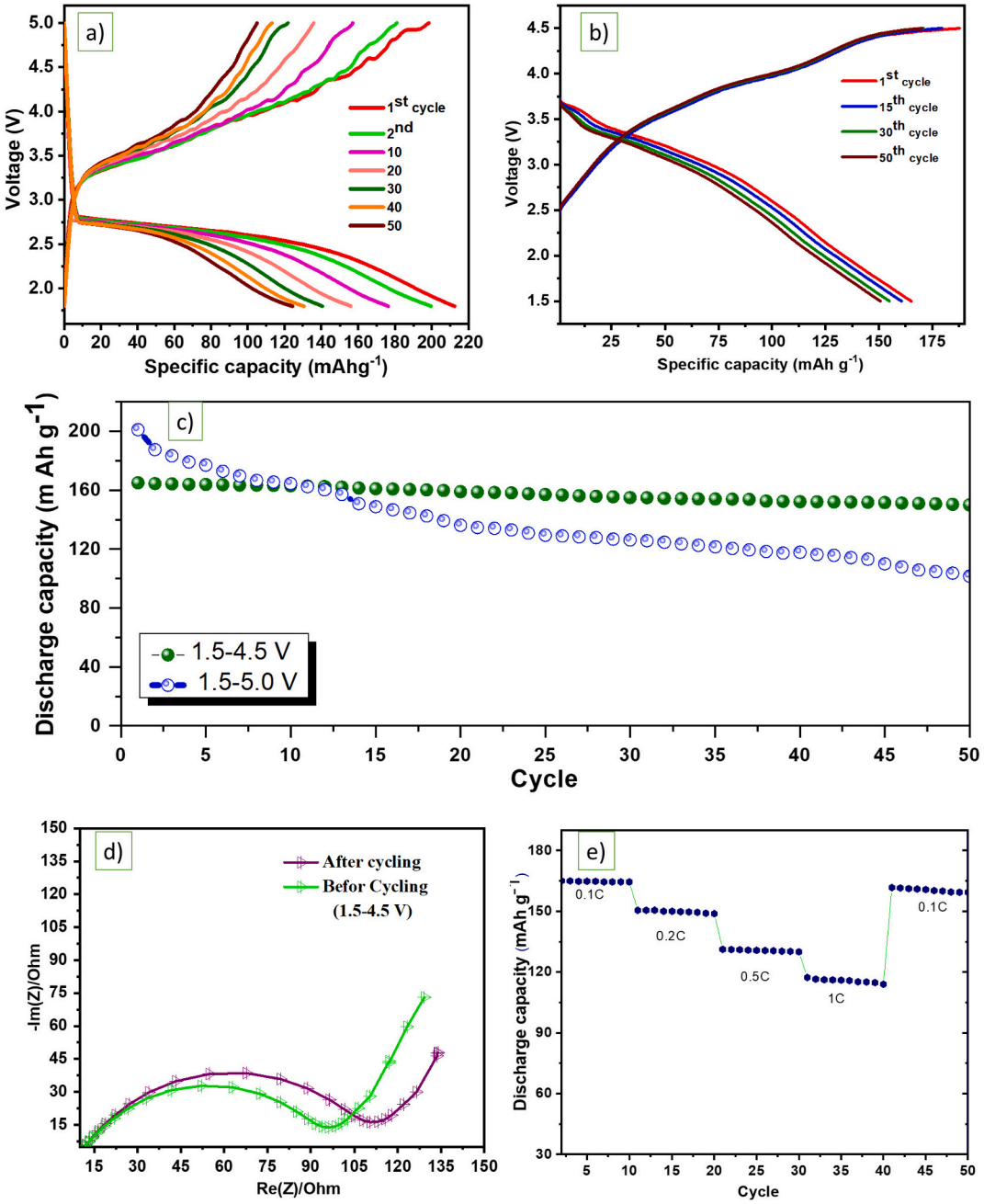

Fig. 4. (a,b) Charge–discharge curves of the P2-NNM material measured in the voltage ranges of 1.5–5.0 V and 1.5–4.5 V at 0.1C, respectively; (c) cyclic stability of P2-NNM at different potential windows; (d) Nyquist plot of the P2-NNM cell before and after cycling within a working voltage of 1.5–4.5 V at 0.1C; and (e) C-rate capability of the P2-NNM electrode in the voltage range of 1.5–4.5 V.

composed of P2-NNM electrodes [40–43]. The rate capability of the material was evaluated at different C-rates ranging from 0.1 to 1.0C, as shown in Fig. 4(e). When the operation was resumed from 1.0C back to 0.1C after successive current rates, the P2-NNM cathode retained a discharge capacity of approximately 158 mAh g^{-1} with no further capacity loss [35,50]. Collectively, these results confirm that the developed P2-NNM material, when paired with an optimized electrolyte, is a promising cathode material for high-voltage and high-capacity sodium-ion battery applications.

To further benchmark the electrochemical performance of the

Table 1
Electrochemical performance comparison of P2- layered oxide cathodes for sodium-ion batteries.

S. No.	Material composition	Structure	Voltage window (V)	Specific capacity (mAh g^{-1})	Cycling performance	Reference
1	$Na_{0.66}Ni_{0.33}Mn_{0.67}O_2$	P2, single crystal	1.5–5.0	218 @ 0.1C	98% Retention after 50 cycles, (4.5 V)	This work
2	$Na_{0.67}Mn_{0.44}Ni_{0.06}Fe_{0.43}Ti_{0.07}O_2$	P2, single crystal	1.5–4.5	186 @ 0.1C	Capacity retention	[3]
3	$Na_{0.67}Ni_{0.33}Mn_{0.67}O_2$ (Nb-doped)	P2, single crystal	1.5–4.5	170 @ 0.1C	Enhanced cycle life (100 cycles)	[8]
4	$Na_{2/3}Ni_{0.23}Al_{0.1}Mn_{2/3}O_{1.95}F_{0.05}$	P2	1.5–4.5	142 @ 0.2C	Good capacity retention	[9]
5	$Na_{0.67}Mn_{0.8}Fe_{0.1}Sb_{0.1}O_2$	P2/O3	1.5–4.3	131 @ 0.1C	Remarkable rate capability	[29]

present P2-NNM cathode, a comparison with representative P2-type layered oxide cathodes reported in the literature is summarized in Table 1.

The comparison in Table 1 demonstrates that the electrochemical performance of the present P2-NNM cathode is on par with or exceeds that of analogous P2-type layered oxide systems reported in the literature, particularly under high-voltage operation, underscoring the advantages of the single-crystal design. The superior electrochemical performance of the P2-NNM cathode can be attributed to several synergistic factors. First, the single-crystal morphology effectively minimizes grain boundaries, which are commonly associated with crack formation and accelerated electrolyte penetration in polycrystalline materials. This structural integrity significantly enhances cycling stability, particularly under high-voltage operation. Second, the P2-type layered framework provides wide Na^{+} diffusion channels, enabling efficient sodium-ion transport and favorable rate performance. In addition, the optimized Ni^{2+}/Ni^{4+} and Mn^{3+}/Mn^{4+} redox couples contribute to high reversible capacity while suppressing severe Jahn–-Teller distortion at MnO_6 octahedral sites. Furthermore, the compatibility between the cathode surface and the optimized electrolyte reduces parasitic side reactions at elevated voltages, collectively resulting in improved capacity retention and electrochemical reversibility.

4. Conclusions

A single-crystal, high-performance P2-type layered $Na_{0.66}Ni_{0.33}Mn_{0.67}O_2$ cathode material was successfully synthesized via a solid-state method without detectable $NiMnO_4$ impurities. This study systematically investigated the electrochemical characteristics of the P2-NNM material, demonstrating a high working potential and a specific discharge capacity exceeding 200 mAh g^{-1} when paired with an optimized electrolyte. The single-crystal P2-NNM cathode exhibited excellent structural stability during electrochemical cycling. Even when operated up to 5.0 V, the material retained its layered structure without significant degradation, highlighting the beneficial role of the single-crystal morphology in mitigating structural damage. Among the investigated voltage windows, the 1.5–4.5 V range delivered superior cycling stability and prolonged lifespan, indicating that both cut-off voltage and electrolyte selection play critical roles in determining electrochemical performance.In the context of renewable energy storage, sodium-ion batteries are increasingly recognized as cost-effective and sustainable alternative for large-scale applications. Recent studies have emphasized the importance of developing structurally stable and high-performance cathode materials to meet the demands of renewable energy integration and grid-scale storage [53–55]. In this regard, the present single-crystal P2-NNM cathode offers a promising pathway toward advanced sodium-ion battery systems for sustainable energy storage. Although the P2-NNM material delivered high capacity at elevated voltages up to 5.0 V, further optimization of the electrolyte is necessary to enhance cycling stability under such high-voltage conditions, particularly for long-term operation in both half-cell and full-cell configurations. Overall, the results demonstrate that single-crystal P2-NNM is a promising high-voltage cathode material for sodium-ion batteries, offering a viable pathway toward improved energy density, durability, and next-generation SIB development. These materials meet the increasing needs of applications like grid energy storage and electric cars by maximizing electrochemical performance, structural stability, and energy eficiency.

CRediT authorship contribution statement

Pavithra Kamatchisundaram: Writing – original draft, Methodology, Formal analysis, Data curation. **Meyyappan Revathi:** Visualization, Validation, Supervision, Conceptualization. **S. Bala Abirami:** Writing – review & editing, Visualization, Validation, Methodology.

Author statement

- All authors have made significant contributions to this manuscript and approve its submission to *Solid State Ionics*. The contributions of each author are as follows: conceptualization and design of the study, data collection, analysis and interpretation, and preparation and revision of the manuscript were carried out collaboratively by the authors.
- The authors confirm that this work is original, has not been published previously, and is not under consideration for publication elsewhere. All authors have read and approved the final version of the manuscript.
- The authors declare that there are no conflicts of interest regarding the publication of this paper. Any financial support received for this work has been duly acknowledged in the manuscript.
- All applicable ethical standards were followed during the course of this research.

Declaration of competing interest

The authors declare no conflict of interest.

Acknowledgments

All the authors from Vels Institute of Science, Technology and Advanced Studies gratefully acknowledge for extending the analytical facilities by the Department of Chemistry, Centre for Alternative Energy & Fuels, VISTAS.

Appendix A. Supplementary data

Supplementary data to this article can be found online at https://doi.org/10.1016/j.ssi.2026.117176.

Data availability

Data will be made available on request.

References

[1] N. Nair, S.V. Nair, S. Baskar, High Na-content P2 and P2-O3 layered oxide cathodes for high performance Na-ion batteries, Mater. Lett. 354 (2024) 135397.
[2] C. Wang, L. Liu, S. Zhao, Y. Liu, Y. Yang, H. Yu, S. Lee, G.H. Lee, Y.M. Kang, R. Liu, F. Li, Tuning local chemistry of P2 layered-oxide cathode for high energy and long cycles of sodium-ion battery, Nat. Commun. 12 (1) (2021) 2256.
[3] B. Kalyoncuoglu, M. Ozgul, S. Altundag, M. Harfouche, E. Oz, S. Avci, X. Ji, S. Altin, M.N. Ates, Unveiling the outstanding full-cell performance of P2-type Na0. 67 (Mn0. 44Ni0. 06Fe0. 43Ti0. 07) O2 cathode active material for Na-ion batteries, J. Power Sources 591 (2024) 233775.
[4] Y. Gupta, P. Siwatch, R. Karwasra, K. Sharma, S.K. Tripathi, Recent progress of layered structured P2-and O3-type transition metal oxides as cathode material for sodium-ion batteries, Renew. Sust. Energ. Rev. 192 (2024) 114167.
[5] P. Arjunan, M. Kouthaman, R. Subadevi, K. Diwakar, W.R. Liu, C.H. Huang, M. Sivakumar, Superior ionic transferring polymer with silicon dioxide composite membrane via phase inversion method designed for high performance sodium-ion battery, Polymers 12 (2) (2020) 405.
[6] D. Hao, G. Zhang, D. Ning, D. Zhou, Y. Chai, J. Xu, X. Yin, R. Du, G. Schuck, J. Wang, Y. Li, Design of high-entropy P2/O3 hybrid layered oxide cathode material for high-capacity and high-rate sodium-ion batteries, Nano Energy 125 (2024) 109562.
[7] W. Yin, Z. Huang, T. Zhang, T. Yang, H. Ji, Y. Zhou, S. Shi, Y. Zhang, P2-type layered oxide cathode with honeycomb-ordered superstructure for sodium-ion batteries, Energy Storage Mater. 69 (2024) 103424.
[8] A. Sengupta, A. Kumar, A. Bano, A. Ahuja, H. Lohani, S.H. Akella, P. Kumari, M. Noked, D.T. Major, S. Mitra, Unleashing the impact of Nb-doped, single crystal, cobalt-free P2-type Na0. 67Ni0. 33Mn0. 67O2 on elevating the cycle life of sodium-ion batteries, Energy Storage Mater. 69 (2024) 103435. https://ui.adsabs.harvard.edu/link_gateway/2024EneSM.6903435S/.
[9] C. Jiang, B. Chen, M. Xu, J. Jiang, Elevating both capacity and voltage tolerance of P2-type layered cathodes with cooperative Al cation/F anion co-doping for advanced sodium-ion batteries, Energy Storage Mater. 70 (2024) 103518.
[10] H. Yang, Q. Zhang, M. Chen, Y. Yang, J. Zhao, Unveiling the origin of air stability in polyanion and layered-oxide cathode materials for sodium-ion batteries and

their practical application considerations, Adv. Funct. Mater. 34 (3) (2024) 2308257.
[11] H. Xu, C. Xie, H. Chen, T. Song, Y. Lan, N. Wu, X. Zhou, P. Kidkhunthod, L. Kang, X. Han, W. Yao, Improving the high-voltage high-rate performance of a P2 layered oxide cathode by a dual-ion doping strategy for sodium-ion batteries, J. Mater. Chem. 12 (2024) 21114.
[12] Q. Liu, Z. Hu, M. Chen, C. Zou, H. Jin, S. Wang, S. Chou, Y. Liu, S. Dou, The cathode choice for commercialization of sodium-ion batteries: layered transition metal oxides versus Prussian blue analogs, Adv. Funct. Mater. 30 (2020) 1909530.
[13] T. Or, S.W. Gourley, K. Kaliyappan, Y. Zheng, M. Li, Z. Chen, Recent progress in surface coatings for sodium-ion battery electrode materials, Electrochem. Energy Rev. 5 (Suppl. 1) (2022) 20.
[14] G. Hao, S.H. Luo, P. Li, G. Wang, W. Zhao, R. Huang, H. Zang, J. Wang, L. Qian, Cu-substituted Na0. 75Ni0. 17Cu0. 08Mn0. 75O2 cathode with suppressing P2-O2 phase transition and air-stable for high-performance sodium-ion batteries, Chem. Eng. J. 496 (2024) 154296, https://doi.org/10.1016/j.cej.2024.154296.
[15] Z. Lv, M. Ling, M. Yue, X. Li, M. Song, Q. Zheng, H. Zhang, J. Energy Chem. 55 (2021) 361 [online].
[16] J. Ding, L. Zhang, X. Li, W. Qiu, Q. Zhu, G. Luo, X. Xiao, J. Nan, X. Zuo, Mechanism of solid electrolyte interphase film formation using ethylene carbonate-based local high concentration electrolyte in sodium-ion batteries, J. Colloid Interface Sci. 685 (2025) 153–164.
[17] S. Li, X. Song, P. Jing, X. Xiao, Y. Chen, Q. Sun, M. Huang, Y. Zhang, G. Li, P. Liu, S. Xu, Trace NaBF4 modulated ultralow-concentration ether electrolyte for durable high-voltage sodium-ion batteries, Adv. Funct. Mater. 35 (2025) 2422491.
[18] W. Tian, G. Lin, S. Yuan, T. Jin, Q. Wang, L. Jiao, Competitive coordination and dual interphase regulation of MOF-modified solid-state polymer electrolytes for high-performance sodium metal batteries, Angew. Chem. Int. Ed. 64 (13) (2025) e202423075.
[19] L. Zhu, M. Wang, S. Xiang, L. Fu, D. Sun, X. Huang, Y. Li, Y. Tang, Q. Zhang, H. Wang, Exceeding three-electron reactions in polyanionic cathode to achieve high-energy density for sodium-ion batteries, ACS Nano 18 (20) (2024) 13073–13083.
[20] H. Ma, B. Zhao, J. Bai, P. Wang, W. Li, Y. Mao, X. Zhu, Z. Sheng, X. Zhu, Y. Sun, Crystallinity tuning of Na3V2 (PO4) 3: unlocking sodium storage capacity and inducing pseudocapacitance behavior, Adv. Sci. 10 (4) (2023) 2203552.
[21] Y. Han, Y. Lei, J. Ni, Y. Zhang, Z. Geng, P. Ming, C. Zhang, X. Tian, J.L. Shi, Y. G. Guo, Q. Xiao, Single-crystalline cathodes for advanced Li-ion batteries: progress and challenges, Small 18 (43) (2022) 2107048.
[22] T. Hu, Q. Ren, W. Ding, S. Luo, Z. Liu, P. He, K. Lei, Z. Jiang, R. Zhang, Z. Ye, Z. Huang, Boron doping: a one-stone-for-two-birds strategy to improve electrochemical performance and air stability of P2-type manganese-based cathode materials for sodium-ion batteries, J. Power Sources 658 (2025) 238303.
[23] Z. Zhu, Y. Zou, X. Fu, R. Fang, Z. Zhao, W. Guo, Y. Sun, S. Zhai, M. Ye, Synergistically stabilized O3-type layered oxide cathodes via phase regulation of multi-cation doping enable high-performance sodium-ion batteries, Appl. Phys. Lett. 127 (9) (2025).
[24] K. Moriya, S. Kumakura, E.J. Kim, Y. Miura, K. Kubota, R. Tatara, S. Komaba, Unique impacts of Scandium doping on electrode performance of P'2-and P2-type Na2/3MnO2, Adv. Mater. 38 (2025) e11719.
[25] X. Dong, X. Wang, Z. Lu, Q. Shi, Z. Yang, X. Yu, W. Feng, X. Zou, Y. Liu, Y. Zhao, Construction of Cu-Zn Co-doped layered materials for sodium-ion batteries with high cycle stability, Chin. Chem. Lett. 35 (5) (2024) 108605.
[26] Y. Zhou, M. Sun, M. Cao, Y. Zeng, M. Su, A. Dou, X. Hou, Y. Liu, Simultaneously promoting the surface/bulk structural stability of Fe/Mn-based layered cathode for sodium ion batteries, J. Colloid Interface Sci. 657 (2024) 472–481.
[27] C. Ren, Y. Dong, Y. Lei, High-voltage cathode materials for sodium-ion batteries: advances and challenges, Small 2025 (2025) 2501262.
[28] G. Wan, B. Peng, L. Zhao, F. Wang, L. Yu, R. Liu, G. Zhang, Dual-strategy modification on P2-Na0. 67Ni0. 33Mn0. 67O2 realizes stable high-voltage cathode and high energy density full cell for sodium-ion batteries, SusMat 3 (1) (2023) 58–71.
[29] S. Jamil, F. Mudasar, T. Yuan, M. Fasehullah, G. Ali, K.H. Chae, O. Voznyy, Y. Zhan, M. Xu, Sb-doped biphasic P2/O3-type Mn-rich layered oxide cathode material for high-performance sodium-ion batteries, ACS Appl. Mater. Interfaces 16 (12) (2024) 14669–14679.
[30] X. Zheng, X. Liu, X. Yang, A. Fu, Y. Li, Y.G. Guo, H. Li, Templating preparation of cannular congeries of MnO2 and porous spheres of carbon and their applications to high performance asymmetric supercapacitor and lithium-sulfur battery, Colloids Surf. A Physicochem. Eng. Asp. 610 (2021) 125740.
[31] V. Pamidi, C. Naranjo, S. Fuchs, H. Stein, T. Diemant, Y. Li, J. Biskupek, U. Kaiser, S. Dinda, A. Reupert, S. Behara, Single-crystal P2–Na0. 67Mn0. 67Ni0. 33O2 cathode material with improved cycling stability for sodium-ion batteries, ACS Appl. Mater. Interfaces 16 (20) (2024) 25953–25965.
[32] Y. Pang, Y. Wang, X. Ding, Y. Xin, Q. Zhou, C. Jiang, B. Chen, H. Liu, F. Wu, H. Gao, A high-entropy approach to activate the oxygen redox activity and suppress the phase transition of P2-type layered cathode for sodium-ion batteries, ACS Sustain. Chem. Eng. 12 (2024) 8203.
[33] H. Liu, N. Hong, N. Bugday, S. Yasar, S. Altin, W. Deng, W. Deng, G. Zou, H. Hou, Z. Long, X. Ji, High voltage Ga-doped P2-type Na2/3Ni0. 2Mn0. 8O2 cathode for sodium-ion batteries, Small 20 (17) (2024) 2307225.
[34] L. Feng, J. Guo, C. Sun, X. Xiao, L. Feng, Y. Hao, G. Sun, Z. Tian, T. Li, Y. Li, Y. Jiang, An active strategy to reduce residual alkali for high-performance layered oxide cathode materials of sodium-ion batteries, Small 20 (2024) 2403084.
[35] Y. Zhu, W. Nie, P. Chen, Y. Zhou, Y. Xu, Li-doping stabilized P2-Li0. 2Na1. 0Mn0. 8O2 sodium ion cathode with oxygen redox activity, Int. J. Energy Res. 44 (4) (2020) 3253–3259.
[36] C. Su, G. Liu, Q. Sun, L. Wen, Z. Chen, M. Zhao, New strategy to build a high-performance P′ 2-type cathode material through oxygen vacancies and Mg substitution for sodium-ion batteries, ACS Appl. Energy Mater. 7 (5) (2024) 1927–1937.
[37] D. Wang, C. Zhu, Y. Liu, C. Hu, H. Yang, Z. Li, T. Chen, B. Zhong, Z. Wu, X. Guo, A feasible dual modification strategy of internal anion redox chemistry and surface engineering on P2 layer-structured cathodes in sodium-ion batteries, ACS Appl. Mater. Interfaces 16 (19) (2024) 24442–24452.
[38] N. Hong, K. Wu, Z. Peng, Z. Zhu, G. Jia, M. Wang, Improved high rate performance and cycle performance of Al-doped O3-type NaNi0. 5Mn0. 5O2 cathode materials for sodium-ion batteries, J. Phys. Chem. C 124 (42) (2020) 22925–22933.
[39] B. Wang, J. Ma, K. Wang, D. Wang, G. Xu, X. Wang, Z. Hu, C.W. Pao, J.L. Chen, L. Du, X. Du, High-entropy phase stabilization engineering enables high-performance layered cathode for sodium-ion batteries, Adv. Energy Mater. 14 (2024) 2401090.
[40] X.B. Jia, J. Wang, Y.F. Liu, Y.F. Zhu, J.Y. Li, Y.J. Li, S.L. Chou, Y. Xiao, Facilitating layered oxide cathodes based on orbital hybridization for sodium-ion batteries: marvelous air stability, controllable high voltage, and anion redox chemistry, Adv. Mater. 36 (15) (2024) 2307938.
[41] M.A.A.M. Abdah, N.H.N. Azman, S. Kulandaivalu, Y. Sulaiman, Review of the use of transition-metal-oxide and conducting polymer-based fibres for high-performance supercapacitors, Mater. Des. 186 (2020) 108199.
[42] A. Massaro, G. Lingua, F. Bozza, A. Piovano, P.P. Prosini, A.B. Muñoz-García, M. Pavone, C. Gerbaldi, P2-type Na0. 84Li0. 1Ni0. 27Mn0. 63O2-layered oxide Na-ion battery cathode: structural insights and electrochemical compatibility with room-temperature ionic liquids, Chem. Mater. 36 (14) (2024) 7046–7055.
[43] J. He, M. Wang, W. Wang, R. Miao, W. Zhong, S.Y. Chen, S. Poges, T. Jafari, W. Song, J. Liu, S.L. Suib, Hierarchical mesoporous NiO/MnO2@ PANI core–shell microspheres, highly efficient and stable bifunctional electrocatalysts for oxygen evolution and reduction reactions, ACS Appl. Mater. Interfaces 9 (49) (2017) 42676–42687.
[44] M. Song, D. Ye, W. Li, C. Lu, W. Wu, X. Wu, Interfacial engineering of P2-type Ni/Mn-based layered oxides by a facile water-washing method for superior sodium–ion batteries, ACS Appl. Mater. Interfaces 16 (13) (2024) 16120–16131.
[45] W. Zuo, A. Innocenti, M. Zarrabeitia, D. Bresser, Y. Yang, S. Passerini, Layered oxide cathodes for sodium-ion batteries: storage mechanism, electrochemistry, and techno-economics, Acc. Chem. Res. 56 (3) (2023) 284–296.
[46] A. Ramesh, A. Tripathi, P. Balaya, A mini review on cathode materials for sodium-ion batteries, Int. J. Appl. Ceram. Technol. 19 (2) (2022) 913–923.
[47] P. Gupta, S. Pushpakanth, M.A. Haider, S. Basu, Understanding the design of cathode materials for Na-ion batteries, ACS Omega 7 (7) (2022) 5605–5614.
[48] M. Ren, S. Zhao, S. Gao, T. Zhang, M. Hou, W. Zhang, K. Feng, J. Zhong, W. Hua, S. Indris, K. Zhang, Homeostatic solid solution in layered transition-metal oxide cathodes of sodium-ion batteries, J. Am. Chem. Soc. 145 (2022) 224–233.
[49] Z. Wu, Y. Ni, S. Tan, E. Hu, L. He, J. Liu, M. Hou, P. Jiao, K. Zhang, F. Cheng, J. Chen, Realizing high capacity and zero strain in layered oxide cathodes via lithium dual-site substitution for sodium-ion batteries, J. Am. Chem. Soc. 145 (17) (2023 Apr 14) 9596–9606.
[50] L. Noerochim, S. Suwarno, N.H. Idris, H.K. Dipojono, Recent development of nickel rich and cobalt-free cathode materials for lithium-ion batteries, Batteries 7 (4) (2021) 84.
[51] W.Z. Liu, Z.Y. Zhou, X.H. Meng, H. Mao, Y. Gong, J.L. Shi, Y.G. Guo, Accomplishing reversible storage of Li-ion beyond stoichiometric 1.1 in Li-rich cathodes via regulating cation migration kinetics, eScience Energy 1 (2025 Oct 30) 100002.
[52] W. Hua, X. Yang, N.P. Casati, L. Liu, S. Wang, V. Baran, M. Knapp, H. Ehrenberg, S. Indris, Probing thermally-induced structural evolution during the synthesis of layered Li-, Na-, or K-containing 3d transition-metal oxides, eScience 2 (2) (2022 Mar 1) 183–191.
[53] L. Li, Q. Chen, M. Jiang, T. Ning, L. Tan, X. Zhang, J. Zheng, J. Wang, Q. Wu, X. Ji, F. Wu, Uncovering mechanism behind tungsten bulk/grain-boundary modification of Ni-rich cathode, Energy Storage Mater. 75 (2025 Feb 1) 104016.
[54] K. Zou, M. Jiang, T. Ning, L. Tan, J. Zheng, J. Wang, X. Ji, L. Li, Thermodynamics-directed bulk/grain-boundary engineering for superior electrochemical durability of Ni-rich cathode, J. Energy Chem. 97 (2024 Oct 1) 321–331.
[55] M. Jiang, P. Wang, Q. Chen, Y. Zhang, Q. Wu, L. Tan, T. Ning, L. Li, K. Zou, Enabling the Nb/Ti co-doping strategy for improving structure stability and rate capability of Ni-rich cathode, Chin. Chem. Lett. 36 (6) (2025 Jun 1) 110040.